COMMUNICATION

Chiral Tetrakis Eu(III) Complexes with Ammonium Cations for Improved Circularly Polarized Luminescence

Makoto Tsurui,[a] Ryohei Takizawa,[a] Yuichi Kitagawa,[b,d] Mengfei Wang,[b,d] Masato Kobayashi,[c,d] Tetsuya Taketsugu[c,d] and Yasuchika Hasegawa*[b,d]

[a] M. Tsurui, R. Takizawa
Graduate School of Chemical Sciences and Engineering, Hokkaido University
Kita 13, Nishi 8, Kita-ku, Sapporo, Hokkaido 060-8628 (Japan).

[b] Dr. Y. Kitagawa, Dr. M. Wang, Prof. Dr. Y. Hasegawa
Faculty of Engineering, Hokkaido University
Kita 13, Nishi 8, Kita-ku, Sapporo, Hokkaido 060-8628 (Japan).
E-mail: hasegaway@eng.hokudai.ac.jp

[c] Dr. M. Kobayashi, Prof. Dr. T. Taketsugu
Faculty of Science, Hokkaido University
Kita 10, Nishi 8, Kita-ku, Sapporo, Hokkaido 060-0810 (Japan).

[d] Dr. Y. Kitagawa, Dr. M. Wang, Dr. M. Kobayashi, Prof. Dr. T. Taketsugu, Prof. Dr. Y. Hasegawa
Institute for Chemical Reaction Design and Discovery (WPI-ICReDD), Hokkaido University
Kita 21, Nishi 10, Kita-ku, Sapporo, Hokkaido 001-0021 (Japan).

Supporting Information for this article is given via a link at the end of the document.

Abstract: Large dissymmetry factor of the circularly polarized luminescence (g_{CPL}) was observed in ligand and coordination tuned chiral tetrakis europium (Eu(III)) complexes with ammonium cations. The g_{CPL} value was estimated to be −1.54, which is the largest among chiral luminescent molecules. Through photophysical measurements, single crystal X-ray structural analyses and quantum chemical calculations, changes in the geometric and electronic structures were observed for a series of chiral tetrakis Eu(III) complexes which enhanced the g_{CPL} value. The emission quantum yield and photosensitized energy transfer efficiencies of chiral Eu(III) complexes with ammonium cations were also larger than that with previous Cs^+. Based on the systematic modifications and analyses for chiral tetrakis Eu(III) complex, effect of the ammonium cation on enhanced CPL brightness is reported.

Chiral luminophores exhibit circularly polarized luminescence (CPL), which originates from the differential emission intensity of left- and right-handed circularly polarized light.[1] The CPL attracts considerable attention for its potential applications in asymmetric photoreactions, plant growth, three-dimensional displays, bio-imaging, and security inks.[2–4] The magnitude of the CPL is described using the dissymmetry factor (g_{CPL}), which is defined by the following equation:

$$g_{CPL} = 2\frac{I_L - I_R}{I_L + I_R} \quad (1)$$

where I_L and I_R are the intensities of left- and right-handed circularly polarized light, respectively.[1b,4c]

In 2017, Isobe reported effective CPL properties of chiral cylindrical molecules (g_{CPL} = −0.152, I_L/I_R = 46/54).[5] Piguet described chiral Cr(III) complexes with relatively large g_{CPL} in 2019 (g_{CPL} = 0.2, I_L/I_R = 55/45).[6] Various types of chiral luminescent molecules have been synthesized.[4,7] At the present stage, the largest g_{CPL} value was achieved for chiral tetrakis(camphorate) Eu(III) complexes with cesium ions in solution (g_{CPL} = 1.38, I_L/I_R = 84/16)[8] and aggregates (g_{CPL} = 1.45, I_L/I_R = 86/14).[9] Recently, we reported that the mixing of ligand-to-metal charge transfer (LMCT) states into the 4f-4f configuration exerts an influence the CPL properties of chiral camphor-based Eu(III) complexes.[10] Optimizing the conditions for the coordination environment and the ligand/metal coupling in chiral tetrakis(camphorate) Eu(III) complexes opens up polarized-luminescent materials with a large g_{CPL} for various future industrial applications.

Systematic modifications and improvements of molecular structure for Eu(III) complex with CPL property lead to open the frontier field of molecule chemistry and advanced photo-science in future. Herein, chiral tetrakis(camphorate) Eu(III) complexes with three chiral ligands and two types of ammonium cations are prepared (**Figure 1a**). Among the six chiral tetrakis(camphorate) Eu(III) complexes, $TEA^+[Eu(+tfc)_4]^-$ (TEA: tetraethylammonium, +tfc: (+)-3-trifluoroacetylcamphorate) exhibits the largest g_{CPL} (g_{CPL} = −1.54, I_L/I_R = 12/88), and allows the detection of the CPL by naked eye. Based on photophysical measurements, single crystal X-ray structural analyses, and quantum chemical calculations, effect of the ammonium cation on enhanced CPL brightness of chiral tetrakis Eu(III) complex is reported.

First, three types of chiral tetrakis(camphorate) Eu(III) complexes with ammonium cations, $TEA^+[Eu(+tfc)_4]^-$, $TEA^+[Eu(+pfc)_4]^-$, and $TEA^+[Eu(+hfc)_4]^-$ (+pfc: (+)-3-pentafluoropropionylcamphorate, +hfc: (+)-3-heptafluorobutyrylcamphorate), were synthesized (**Figure 1b**).[7m] Single crystals of $TEA^+[Eu(+tfc)_4]^-$ and $TEA^+[Eu(+hfc)_4]^-$ suitable for X-ray diffraction measurements were obtained by recrystallization of an acetonitrile solution of these complexes. The crystal structure and crystallographic data are summarized in **Figure 1c** ($TEA^+[Eu(+tfc)_4]^-$), **1d** ($TEA^+[Eu(+hfc)_4]^-$), and **Table S1** in the Supporting Information.[11] These chiral Eu(III) complexes have eight-coordinate structures in which four chiral camphorate ligands are coordinated to one Eu(III) ion. One ammonium cation is present in the tetrakis(camphorate) Eu(III) unit. Several CH…F interactions between the fluorine atoms in

the ligands and the ammonium cations were observed. Shape measure calculations were performed to evaluate the geometrical structures around the Eu(III) ion (**Table S2** in the Supporting Information).[12] The coordination geometries of these complexes are classified as square antiprism (SAP) structure. The configuration of the camphorate ligands in $TEA^+[Eu(+tfc)_4]^-$ is categorized as Λ-form. On the other hand, four fluoroalkyl chains in $TEA^+[Eu(+hfc)_4]^-$ were oriented toward the ammonium cation, which promoted the formation of the Δ-configuration. The orientation of the chiral Eu(III) complexes was characterized by the length of the fluoroalkyl chains.

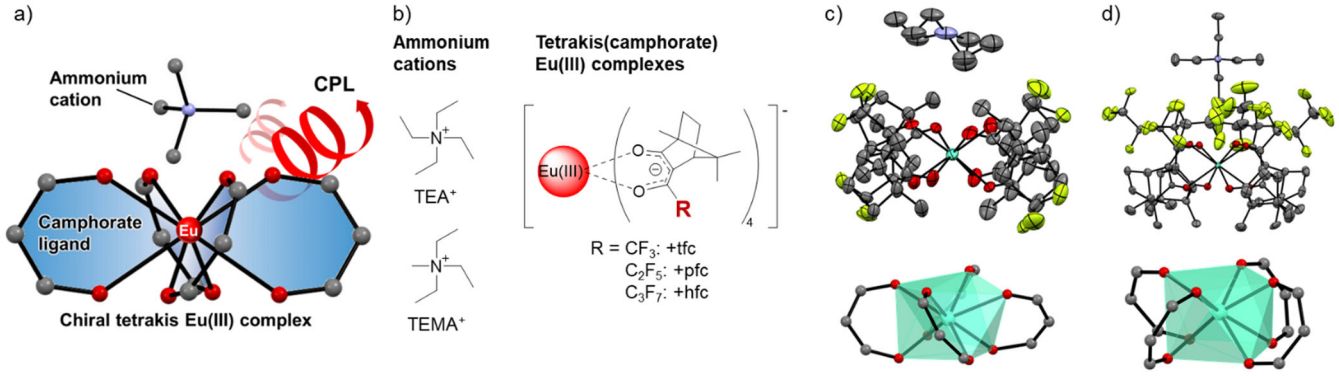

Figure 1. a) Conceptual design of this work. b) Chemical structures of the chiral Eu(III) complexes with ammonium cations. c, d) ORTEP drawings (top, ellipsoids are set at 50 % probability. Hydrogen atoms and solvent molecules are omitted for clarity) and coordination geometries (bottom) of c) $TEA^+[Eu(+tfc)_4]^-$ (Λ-form) and d) $TEA^+[Eu(+hfc)_4]^-$ (Δ-form).

The absorption and circular dichroism (CD) spectra of the Eu(III) complexes in chloroform solutions are shown in **Figure 2a**. The absorption maxima are located at around 310 nm, corresponding to the π − π* transitions of the camphorate ligands. In the CD spectra, $TEA^+[Eu(+tfc)_4]^-$ (with Λ-form) and $TEA^+[Eu(+hfc)_4]^-$ (with Δ-form) showed mirror images. These CD signals reflect the differences in the Δ- and Λ-form of the crystal structure. Additionally, the CD signals of $TEA^+[Eu(+pfc)_4]^-$ were similar to those of $TEA^+[Eu(+hfc)_4]^-$, suggesting that the conformation of $TEA^+[Eu(+pfc)_4]^-$ was classified as the Δ-form. The emission spectra of the chiral Eu(III) complexes showed characteristic sharp bands based on the 4f-4f transitions ($^5D_0 \rightarrow {}^7F_J$, J = 0-4) of the Eu(III) ions (**Figure 2b**).[13] The sharper and slight red shift of emission bands of TEA+$[Eu(tfc)_4]^-$ are based on the geometric structure. Shape measure calculation ratio between SAP and TDH (trigional dodecahedron) of $TEA^+[Eu(tfc)_4]^-$ and $TEA^+[Eu(hfc)_4]^-$, S_{SAP}/S_{TDH} values, were estimated to be 0.55 and 0.19, respectively (Supporting Information Table S2). The large S_{SAP}/S_{TDH} value of $TEA^+[Eu(tfc)_4]^-$ provides structure of distorted SAP structure of the coordination geometry. The emission bands of $TEA^+[Eu(pfc)_4]^-$ agree with those of $TEA^+[Eu(hfc)_4]^-$, resulting in the same coordination geometry as $TEA^+[Eu(hfc)_4]^-$ in liquid media. We consider that the emission spectral shapes are influenced by their coordination geometry ratio of S_{SAP}/S_{TDH}.

The photophysical parameters calculated from the emission spectra and emission lifetimes (τ_{obs}) are summarized in **Table 1** (for calculation method, see the Supporting Information). The calculated intrinsic emission quantum yields ($\Phi_{f\text{-}f}$) of $TEA^+[Eu(+tfc)_4]^-$, $TEA^+[Eu(+pfc)_4]^-$, and $TEA^+[Eu(+hfc)_4]^-$ were found to be 17, 16, and 13%, respectively. Their values are larger than that of previously reported $Cs^+[Eu(hfc)_4]^-$. The large $\Phi_{f\text{-}f}$ of chiral Eu(III) complexes with alkyl-ammonium cation is due to their smaller non-radiative rate constants. The photosensitized energy transfer efficiencies (η_{sens}) of chiral Eu(III) complexes with TEA and TEMA cations (39 - 61%) were also larger than that of $Cs^+[Eu(hfc)_4]^-$ (29%).

In the CPL spectra of $TEA^+[Eu(+tfc)_4]^-$, large negative (580 - 600 nm) and positive (605 - 620 nm) signals were contributed by the $^5D_0 \rightarrow {}^7F_1$ and $^5D_0 \rightarrow {}^7F_2$ transitions, respectively (**Figure 2b**). The g_{CPL} of $TEA^+[Eu(+tfc)_4]^-$ corresponding to the $^5D_0 \rightarrow {}^7F_1$ transition (594 nm) was calculated to be −1.54, which is the largest $|g_{CPL}|$ value among reported chiral Eu(III) complexes. The large difference between I_L and I_R (I_L/I_R = 12/88) allows detection of the CPL by the naked eye using a digital camera equipped with bandpass filter (590 nm, FWHM: 10 nm), rotatable λ/4 plate, and linear polarizer (**Figure 2c**).[4d] The g_{CPL} values of $TEA^+[Eu(+pfc)_4]^-$ and $TEA^+[Eu(+hfc)_4]^-$ were estimated to be +1.28 and +1.45, respectively. We also prepared chiral Eu(III) complexes with $TEMA^+$ (TEMA: triethylmethylammonium), $TEMA^+[Eu(+tfc)_4]^-$, $TEMA^+[Eu(+pfc)_4]^-$, and $TEMA^+[Eu(+hfc)_4]^-$. The CPL properties of these complexes are also summarized in **Table 2**. The g_{CPL} value of $TEMA^+[Eu(+tfc)_4]^-$ was also larger than those of $TEMA^+[Eu(+pfc)_4]^-$, and $TEMA^+[Eu(+hfc)_4]^-$.

CPL performance of chiral Eu(III) complex is estimated using the CPL brightness with absorption transition process and the emission quantum yield.[13] The CPL brightness B_{CPL} is given by,

$$B_{CPL} = \beta_i \times \varepsilon_\lambda \times \phi \times \frac{|g_{CPL}|}{2}, \beta_i = \frac{I_i}{\sum_j I_j} \quad (2),$$

where ε_λ and ϕ are extinction coefficient and emission quantum yield at the excitation wavelength, respectively. The I_i is the integrated intensity of the considered transition and $\sum_j I_j$ is the summation of the integrated intensities over all the transitions.[13]

Table 1. Photophysical parameters of chiral Eu(III) complexes in 2 mM chloroform solution.

Compounds	τ_{obs}[a] / ms	$\Phi_{\pi\text{-}\pi}$[b] / % ($^5D_0 \rightarrow {}^7F_{0\text{-}4}$)	$\Phi_{f\text{-}f}$ / % ($^5D_0 \rightarrow {}^7F_{0\text{-}4}$)	k_r / s^{-1}	k_{nr} / s^{-1}	η_{sens} / %
$TEA^+[Eu(+tfc)_4]^-$	0.371	8.2	17	4.7×10^2	2.2×10^3	48
$TEA^+[Eu(+pfc)_4]^-$	0.317	6.3	16	5.0×10^2	2.7×10^3	39
$TEA^+[Eu(+hfc)_4]^-$	0.263	5.8	13	4.8×10^2	3.3×10^3	45
$TEMA^+[Eu(+tfc)_4]^-$	0.367	10.3	17	4.7×10^2	2.3×10^3	61
$TEMA^+[Eu(+pfc)_4]^-$	0.345	8.3	17	5.0×10^2	2.4×10^3	49
$TEMA^+[Eu(+hfc)_4]^-$	0.332	7.5	16	4.7×10^2	2.5×10^3	47
$Cs^+[Eu(+hfc)_4]^-$	0.204	2.6	9	4.4×10^2	4.5×10^3	29

[a] Emission lifetimes were determined by fitting the emission decay curves to a single exponential function (**Figure S4** in the Supporting Information). Excited at 355 nm. [b] Excited at 370 nm. 1 mM.

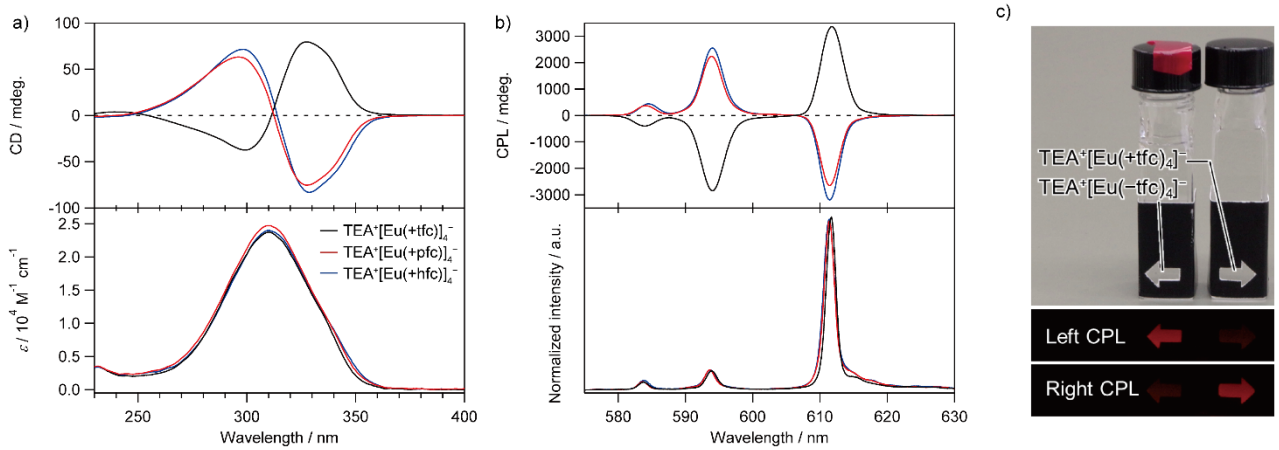

Figure 2. a) CD (top, 0.2 mM) and absorption (bottom, 0.2 mM), and b) CPL (top, 2 mM, λ_{ex} = 350 nm) and emission (bottom, 2 mM, λ_{ex} = 360 nm) spectra of $TEA^+[Eu(+tfc)_4]^-$ (black), $TEA^+[Eu(+pfc)_4]^-$ (red), and $TEA^+[Eu(+hfc)_4]^-$ (blue) in chloroform solution. c) Photographs of the emission of $TEA^+[Eu(+tfc)_4]^-$ (right) and $TEA^+[Eu(-tfc)_4]^-$ (left) in 2 mM chloroform solution. Under room light (top, without any optical filter), left (middle) and right (bottom) circularly polarized light (λ_{ex} = 365 nm).

These calculations are assumption under excitation-independent $\Phi_{\pi\text{-}\pi}$ and g_{CPL}.

Calculated B_{CPL} values of chiral tetrakis Eu(III) complexes are shown in Table 2. The CPL brightness (B_{CPL}) at $^5D_0 \rightarrow {}^7F_1$ transition of $TEA^+[Eu(+tfc)_4]^-$ (g_{CPL} = −1.54, B_{CPL} = 223 $M^{-1}cm^{-1}$) is greater than that of the previously reported $Cs^+[Eu(+hfc)_4]^-$ (g_{CPL} = +1.38,[8] B_{CPL} = 66 $M^{-1}cm^{-1}$). The enhancement of CPL properties (g_{CPL}, B_{CPL}) is achieved through a two-step strategy: first, $Cs^+[Eu(+hfc)_4]^- \rightarrow TEA^+[Eu(+hfc)_4]^-$ (g_{CPL} = −1.45, B_{CPL} = 142 $M^{-1}cm^{-1}$) by replacing Cs^+ with TEA^+, and then $TEA^+[Eu(+hfc)_4]^- \rightarrow TEA^+[Eu(+tfc)_4]^-$ by substituting +hfc with +tfc ligand. In contrast to Cs^+, which interacts with the +hfc ligand through both coordinate bonds with oxygen atoms and the CF…Cs^+ electrostatic interactions,[8,14] and TEA^+ is located above the +hfc ligand involved with the CH…F interactions. Achieving a balance between the interaction of the counter cation with the tetrakis europium anion and the ligand/metal coupling proves crucial for enhancing CPL properties. Therefore, we realized the improvement of CPL in the chiral tetrakis Eu(III) luminophore, attached with TEA^+ and +tfc ligand.

According to the Rosenfeld equation, rotational strength parameter of CPL depends on the scalar product of the magnetic dipole (MD) transition moment vector and an electric dipole (ED) transition moment vector.[15] At the present time, transition moment vectors of MD and ED of chiral Eu(III) complexes cannot be estimated, experimentally. The quantum chemical estimation of their transition moment vectors in Eu(III) complexes in liquid media are expected to well-understand the CPL mechanism.

Here, we consider effect of the LMCT on CPL properties. TD-DFT calculations were performed using structures optimized at the ground state (Figure S5, Table S3 - S8 in the Supporting Information). Four LMCT excited states were calculated for each Eu(III) complex (Tables S9 - S17: TD-DFT calculations based on the optimized structure using SMD solvation model, Tables S18 – S20: TD-DFT calculations based on the crystal structure in the Supporting Information). These tables include excitation energies, magnitudes of electric and magnetic transition dipole moments ($|\boldsymbol{\mu}|$ and $|\boldsymbol{m}|$), the angles between them (θ), and the g_{CPL} values, estimated by the following equation:

$$g_{\mathrm{CPL}} = 4\frac{|\boldsymbol{\mu}||\boldsymbol{m}|\cos\theta}{|\boldsymbol{\mu}|^2+|\boldsymbol{m}|^2} \quad (3).$$

Additionally, the ligand orbitals primarily involved in each LMCT excitation are provided. It is important to note that these

excited eigenstates do not directly influence the f-f emission properties. However, LMCT configurations mixed into the f-f excited state can perturb the electric and magnetic transition dipole moments. For comparison, properties related to f-f transitions are also listed in Table S12. Typically, the magnitudes of electric transition dipoles for LMCT states are larger than those for f-f states, which are dipole forbidden, while the revise is true for magnetic dipoles. Among the four LMCT excited states, the second and third states exhibit larger electronic transition dipoles than the first and fourth states. This variance is associated with the ligand orbitals involved in the LMCT transition. In tetrakis ligands, two ligands opposite each other across the Eu atom pair up, sharing similar Eu-O distances, which mixes the π orbitals of each ligand pair, resulting in either the first two or the latter two ligand orbitals involved in the LMCT transition. Due to the SAP structure of the ligands, which are approximately perpendicular to each other, the energy difference between the two ligand-pair orbitals (one being an in-phase and the other an inverse-phase mixture) is small (Supporting Information Figure S12 – S17). The dipole integral $\langle \Psi_{\mathrm{LMCT}}|\alpha|\Psi_0\rangle = \langle \phi_{\mathrm{ligand}}|\alpha|\phi_{4\mathrm{f}}\rangle$ $(\alpha = x, y, \text{or } z)$ for one of these two ligand-to-4f transitions becomes significant, while it is approximately forbidden for the opposite transition. The incorporation of an allowed LMCT configuration into the f-f excited state may increase the electric transition dipole moment, thus influencing the g_{CPL} value. The increase of the electric transition dipole moment is also supported by previous reports. Hatanaka demonstrated that $^5D_0 \rightarrow {}^7F_2$ transition is sensitive to mixing of LMCT states.[16] The CPL characteristics of the $^5D_0 \rightarrow {}^7F_1$ transition can be affected by LMCT perturbation through the J-mixing effect.[7n,17]

In summary, CPL brightness of chiral tetrakis(camphorate) Eu(III) complexes were improved by addition of alkyl-ammonium cation. The alkyl-ammonium cation promotes enhancement of dissymmetry factor g_{CPL}, 4f-4f and photosensitized emission quantum yields. The large CPL brightness of chiral tetrakis Eu(III) complexes with ammonium cation are expected to be useful for CPL performance under UV lamp or UV-LED irradiation. Further systematic evaluation of quantum chemical calculations of chiral tetrakis(camphorate) Eu(III) complexes should open-up well-understandings the CPL mechanism of chiral lanthanide complex. These photophysical findings will provide further development of chiral Eu(III) complexes with strong CPL characteristics for application in next-generation luminescent materials.

Table 2. Circularly polarized luminescence parameters of chiral Eu(III) complexes in chloroform solution.

Compounds	$\varepsilon_{\max}$ / $\mathrm{cm^{-1}M^{-1}}$ [a]	^7F_J	g_{CPL} [b]	β_i	B_{CPL} [d] / $\mathrm{M^{-1}cm^{-1}}$
$TEA^+[Eu(+tfc)_4]^-$	38,000	$J = 1$	−1.54	0.093	223
		$J = 2$	+0.23	0.53	190
$TEA^+[Eu(+pfc)_4]^-$	36,000	$J = 1$	+1.28	0.088	128
		$J = 2$	−0.18	0.53	108
$TEA^+[Eu(+hfc)_4]^-$	37,000	$J = 1$	+1.45	0.091	142
		$J = 2$	−0.22	0.54	127
$TEMA^+[Eu(+tfc)_4]^-$	38,000	$J = 1$	−1.49	0.095	277
		$J = 2$	+0.19	0.57	212
$TEMA^+[Eu(+pfc)_4]^-$	36,000	$J = 1$	+1.21	0.092	166
		$J = 2$	−0.18	0.54	145
$TEMA^+[Eu(+hfc)_4]^-$	37,000	$J = 1$	+1.46	0.093	188
		$J = 2$	−0.23	0.52	166
$Cs^+[Eu(+hfc)_4]^-$	37,000	$J = 1$	+1.38 [c]	0.099	66
		$J = 2$	−0.23 [c]	0.51	56

[a] The $\varepsilon_{\max}$ for $[Eu(+tfc)_4]^-$ with TEA^+ and $TEMA^+$, $[Eu(+pfc)_4]^-$ with TEA^+ and $TEMA^+$ and $[Eu(+hfc)_4]^-$ with TEA^+, $TEMA^+$ and Cs^+ are estimated by absorption measurements of $TEMA^+[Eu(+tfc)_4]^-$, $TEA^+[Eu(+pfc)_4]^-$ and $TEMA^+[Eu(+hfc)_4]^-$, respectively. [b] λ_{ex} = 350 nm, [c] Ref. 8. [d] The $\Phi_{\pi\text{-}\pi}$ in Table 1 (λ_{ex} = 370 nm) is used as ϕ value in equation 2 for calculation of B_{CPL}. These calculations are assumption under excitation-independent $\Phi_{\pi\text{-}\pi}$ and g_{CPL}.

Supporting Information

The authors have cited additional references within the Supporting Information.[18–27]

Acknowledgements

This work was supported by JSPS KAKENHI Grant Numbers JP22H02152 (Y. H.), JP22H04516 (Y. H.), JP23K17925(Y. H.), JP23H04863 (Y. K.), and JP21K18969 (Y. K.). This work was also supported by Grant-in-Aid for JSPS Fellows Grant Number JP22KJ0021 (M. T.) and the Institute for Chemical Reaction Design and Discovery (ICReDD), established by the World Premier International Research Center Initiative (WPI).

Keywords: chirality • circularly polarized luminescence • europium • lanthanides

[1] a) F. S. Richardson, J. P. Riehl, F. S. Richardson, J. P. Riehl, *Chem. Rev.* **1977**, *77*, 773–792; b) S. F. Mason, *Molecular Optical Activity and the Chiral Discriminations*, Cambridge University Press, **1982**; c) J. P. Riehl, F. S. Richardson, *Chem. Rev.* **1986**, *86*, 1–16.

[2] a) T. Kawasaki, M. Sato, S. Ishiguro, T. Saito, Y. Morishita, I. Sato, H. Nishino, Y. Inoue, K. Soai, *J. Am. Chem. Soc.* **2005**, *127*, 3274–3275; b) J. S. Kang, S. Kang, J.-M. Suh, S. M. Park, D. K. Yoon, M. H. Lim, W. Y. Kim, M. Seo, *J. Am. Chem. Soc.* **2022**, *144*, 2657–2666; c) L. E. MacKenzie, R. Pal, *Nat. Rev. Chem.* **2020**, *5*, 109–124; d) E. Lkhamkhuu, K. Zikihara, H. Katsura, S. Tokutomi, T. Hosokawa, Y. Usami, M. Ichihashi, J. Yamaguchi, K. Monde, *Plant Biotechnol.* **2020**, *37*, 57–67.

[3] a) Y. Sang, J. Han, T. Zhao, P. Duan, M. Liu, *Adv. Mater.* **2020**, *32*, 1900110; b) F. Zinna, M. Pasini, F. Galeotti, C. Botta, L. Di Bari, U. Giovanella, *Adv. Funct. Mater.* **2017**, *27*, 1603719; c) F. Song, Z. Xu, Q. Zhang, Z. Zhao, H. Zhang, W. Zhao, Z. Qiu, C. Qi, H. Zhang, H. H. Y. Sung, I. D. Williams, J. W. Y. Lam, Z. Zhao, A. Qin, D. Ma, B. Z. Tang, *Adv. Funct. Mater.* **2018**, *28*, 1–12.

[4] a) G. Muller, *Dalton Trans.* **2009**, 9692–9707; b) R. Carr, N. H. Evans, D. Parker, *Chem. Soc. Rev.* **2012**, *41*, 7673–7686; c) F. Zinna, L. Di Bari, *Chirality* **2015**, *27*, 1–13; d) Y. Kitagawa, S. Wada, M. D. J. Islam, K. Saita, K. Tanaka, S. Maeda, Y. Hasegawa, *Commun. Chem.* **2020**, *3*, 119–123.

[5] S. Sato, A. Yoshii, S. Takahashi, S. Furumi, M. Takeuchi, H. Isobe, *Proc. Natl. Acad. Sci. U. S. A.* **2017**, *114*, 13097–13101.

[6] J. R. Jiménez, B. Doistau, C. M. Cruz, C. Besnard, J. M. Cuerva, A. G. Campaña, C. Piguet, *J. Am. Chem. Soc.* **2019**, *141*, 13244–13252.

[7] a) J.-Q. Wang, X.-N. Han, Y. Han, C.-F. Chen, *Chem. Commun.* **2023**, *59*, 13089–13106; b) M. Poncet, A. Benchohra, J. Jiménez, C. Piguet, *ChemPhotoChem* **2021**, *5*, 880–892; c) E. S. Gauthier, L. Abella, N. Hellou, B. Darquié, E. Caytan, T. Roisnel, N. Vanthuyne, L. Favereau, M. Srebro-Hooper, J. A. G. Williams, J. Autschbach, J. Crassous, *Angew. Chemie Int. Ed.* **2020**, *59*, 8394–8400; d) N. Saleh, C. Shen, J. Crassous, *Chem. Sci.* **2014**, *5*, 3680; e) S.-Y. Li, L. Xu, R.-T. Gao, Z. Chen, N. Liu, Z.-Q. Wu, *J. Mater. Chem. C* **2023**, *11*, 1242–1250; f) Y. Kitagawa, M. Tsurui, Y. Hasegawa, *ACS Omega* **2020**, *5*, 3786–3791; g) O. G. Willis, F. Zinna, G. Pescitelli, C. Micheletti, L. Di Bari, *Dalton Trans.* **2022**, *51*, 518–523; h) D. Cotter, S. Dodder, V. J. Klimkowski, T. A. Hopkins, *Chirality* **2019**, *31*, 301–311; i) B.-A. N. Willis, D. Schnable, N. D. Schley, G. Ung, *J. Am. Chem. Soc.* **2022**, *144*, 22421–22425; j) H. Tanaka, Y. Inoue, T. Mori, *ChemPhotoChem* **2018**, *2*, 386–402; k) E. M. Sánchez-Carnerero, A. R. Agarrabeitia, F. Moreno, B. L. Maroto, G. Muller, M. J. Ortiz, S. de la Moya, *Chem. – A Eur. J.* **2015**, *21*, 13488–13500; l) M. Hasegawa, Y. Nojima, Y. Mazaki, *ChemPhotoChem* **2021**, *5*, 1042–1058; m) Z. Li, K. Nakamura, N. Kobayashi, *J. Mater. Chem. C* **2023**, *11*, 118–126; n) S. Wada, Y. Kitagawa, T. Nakanishi, M. Gon, K. Tanaka, K. Fushimi, Y. Chujo, Y. Hasegawa, *Sci. Rep.* **2018**, *8*, 16395.

[8] a) J. L. Lunkley, D. Shirotani, K. Yamanari, S. Kaizaki, G. Muller, *J. Am. Chem. Soc.* **2008**, *130*, 13814–13815; b) S. Di Pietro, L. Di Bari, *Inorg. Chem.* **2012**, *51*, 12007–12014.

[9] J. Kumar, B. Marydasan, T. Nakashima, T. Kawai, J. Yuasa, *Chem. Commun.* **2016**, *52*, 9885–9888.

[10] a) M. Tsurui, Y. Kitagawa, S. Shoji, H. Ohmagari, M. Hasegawa, M. Gon, K. Tanaka, M. Kobayashi, T. Taketsugu, K. Fushimi, Y. Hasegawa, *J. Phys. Chem. B* **2022**, *126*, 3799–3807; b) M. Tsurui, Y. Kitagawa, S. Shoji, K. Fushimi, Y. Hasegawa, *Dalton Trans.* **2022**, *52*, 796–805.

[11] Deposition numbers 2329097 (for $TEA^+[Eu(+tfc)_4]^-$), 2329098 (for $TEA^+[Eu(+hfc)_4]^-$), 2329099 (for $TEMA^+[Eu(+hfc)_4]^-$), contain the supplementary crystallographic data for this paper. These data are provided free of charge by the joint Cambridge Crystallographic Data Centre and Fachinformationszentrum Karlsruhe Access Structures service.

[12] a) D. Casanova, M. Llunell, P. Alemany, S. Alvarez, *Chem. Eur. J.* **2005**, *11*, 1479–1494; b) M. Pinsky, D. Avnir, *Inorg. Chem.* **1998**, *37*, 5575–5582; c) "Universitat de Barcelona, 'Electronic Structure Group - SHAPE 2.1', http://www.ee.ub.edu/," **2013**.

[13] L. Arrico, L. Di Bari, F. Zinna, *Chem. Eur. J.* **2021**,*27*, 2920-2934.

[14] J. L. Lunkley, D. Shirotani, K. Yamanari, S. Kaizaki, G. Muller, *Inorg. Chem.* **2011**, *50*, 12724–12732.

[15] R. Carr, R. Puckrin, B. K McMahon, R. Pal, D. Parker, L.-O. Pålsson, *Methods Appl. Fluoresc.* **2014**, 2, 024007.

[16] M. Hatanaka, S. Yabushita, *J. Phys. Chem. A* **2009**, *113*, 12615–12625.

[17] K. Binnemans, *Coord. Chem. Rev.* **2015**, *295*, 1–45.

[18] M. H. V. Werts, R. T. F. Jukes, J. W. Verhoeven, *Phys. Chem. Chem. Phys.* **2002**, *4*, 1542–1548.

[19] G. M. Sheldrick, *Acta Crystallogr. Sect. A Found. Crystallogr.* **2008**, *64*, 112–122.

[20] O. V. Dolomanov, L. J. Bourhis, R. J. Gildea, J. A. K. Howard, H. Puschmann, *J. Appl. Crystallogr.* **2009**, *42*, 339–341.

[21] a) M. J. Frisch, G. W. Trucks, H. B. Schlegel, G. E. Scuseria, M. A. Robb, J. R. Cheeseman, G. Scalmani, V. Barone, G. A. Petersson, H. Nakatsuji, X. Li, M. Caricato, A. V. Marenich, J. Bloino, B. G. Janesko, R. Gomperts, B. Mennucci, H. P. Hratchian, J. V. Ortiz, A. F. Izmaylov, J. L. Sonnenberg, Williams, F. Ding, F. Lipparini, F. Egidi, J. Goings, B. Peng, A. Petrone, T. Henderson, D. Ranasinghe, V. G. Zakrzewski, J. Gao, N. Rega, G. Zheng, W. Liang, M. Hada, M. Ehara, K. Toyota, R. Fukuda, J. Hasegawa, M. Ishida, T. Nakajima, Y. Honda, O. Kitao, H. Nakai, T. Vreven, K. Throssell, J. A. Montgomery Jr., J. E. Peralta, F. Ogliaro, M. J. Bearpark, J. J. Heyd, E. N. Brothers, K. N. Kudin, V. N. Staroverov, T. A. Keith, R. Kobayashi, J. Normand, K. Raghavachari, A. P. Rendell, J. C. Burant, S. S. Iyengar, J. Tomasi, M. Cossi, J. M. Millam, M. Klene, C. Adamo, R. Cammi, J. W. Ochterski, R. L. Martin, K. Morokuma, O. Farkas, J. B. Foresman, D. J. Fox, **2016**, Gaussian 16, Revision C.01, Gaussian, Inc., Wallingford; b) A. V. Marenich, C. J. Cramer, D. G. Truhlar, *J. Phys. Chem. B* **2009**, *113*, 6378–6396.

[22] M. Dolg, H. Stoll, A. Savin, H. Preuss, *Theor. Chim. Acta* **1989**, *75*, 173–194.

[23] B. P. Pritchard, D. Altarawy, B. Didier, T. D. Gibson, T. L. Windus, *J. Chem. Inf. Model.* **2019**, *59*, 4814–4820.

[24] T. H. Dunning, *J. Chem. Phys.* **1989**, *90*, 1007–1023.

[25] A. V. Marenich, C. J. Cramer, D. G. Truhlar, *J. Phys. Chem. B* **2009**, *113*, 6378–6396.

[26] M. Tsurui, Y. Kitagawa, S. Shoji, K. Fushimi, Y. Hasegawa, *Dalton Trans.* **2022**, *52*, 796–805.

[27] M. Pinsky, D. Avnir, *Inorg. Chem.* **1998**, *37*, 5575–5582.

Entry for the Table of Contents

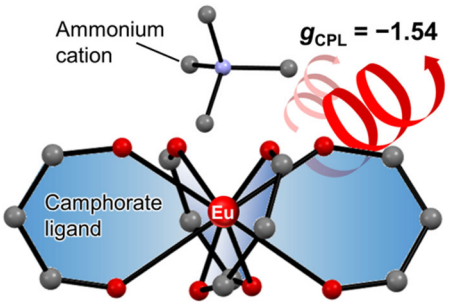

Chiral tetrakis Eu(III) complex

Chiral tetrakis Eu(III) complexes with ammonium cations exhibited large dissymmetry factor of the circularly polarized luminescence (g_{CPL} = −1.54), which is the largest among chiral luminescent molecules. Based on the systematic modifications and analyses for chiral tetrakis Eu(III) complex, effect of the ammonium cation on enhanced CPL brightness is reported.